Sox9-expressing cells promote regeneration after radiation-induced lung injury via PI3K/AKT pathway

Shuang Chen
Sun Yat-sen University First Affiliated Hospital
Kang Li
Sun Yat-sen University First Affiliated Hospital
Xinqi Zhong
Third Affiliated Hospital of Guangzhou Medical College
Ganping Wang
Sun Yat-sen University First Affiliated Hospital
Xiaocheng Wang
Sun Yat-sen University First Affiliated Hospital
Maosheng Cheng
Sun Yat-sen University First Affiliated Hospital
Jie Chen
Sun Yat-sen University First Affiliated Hospital
Zhi Chen
Sun Yat-sen University First Affiliated Hospital
Jianwen Chen
Sun Yat-sen University First Affiliated Hospital
Caihua Zhang
Sun Yat-sen University First Affiliated Hospital
Gan Xiong
Sun Yat-Sen University Guanghua School of Stomatology,hospital of stomatology
Xiuyun Xu
Sun Yat-Sen University Guanghua School of Stomatology, hospital of stomatology
Demeng Chen (chendm29@mail.sysu.edu.cn)
Sun Yat-sen University First Affiliated Hospital
Heping Li
Sun Yat-sen University First Affiliated Hospital
Liang Peng
Chinese PLA General Hospital

Research Article

Keywords: radiation induced lung injury, Sox9, lineage tracing assay

Posted Date: March 4th, 2021

DOI: https://doi.org/10.21203/rs.3.rs-261497/v1

Abstract

Background

Radiation induced lung injury (RILI) is considered as one of the most common complications of thoracic radiation. Recent studies have focused on stem cells properties to obtain ideal therapeutic effects and Sox9 has been reported to be involved in stem cell induction and differentiation. However, whether Sox9-expressing cells play a role in radiation repair and regeneration remain unknown.

Methods

We successfully obtain SOX9^{CreER}, Rosa^{tdTomato} and Rosa^{DTA} mice and identify Sox9-expressing cells through lineage tracing assay. Then we evaluated the effects of the ablation of Sox9-expressing cells in vivo. Furthermore, we investigated the underlying mechanism of Sox9 expressing cells during lung regeneration via an online single cell RNA-seq dataset.

Results

In our study, we demonstrated Sox9-expressing cells promote regenerative of lung tissues and ablation of Sox9-expressing cells leads to severe phenotypes after radiation damage. In addition, analysis of online scRNA-seq dataset revealed an enrichment of PI3K/AKT pathway in Sox9-expressing cells during lung epithelium regeneration. Finally, AKT inhibitor Perifosine could suppress the regenerative effects of Sox9-expressing cells.

Conclusions

Taken together, our study suggests that Sox9-expressing cells may serve as a therapeutic target in the setting of lung tissue after RILI.

1. Introduction

About 4.3 million (Thoracic cancer) new cancer cases and 2.9 million deaths were reported in China alone in 2018 and most of which had unresectable disease (Feng et al., 2019). Radiotherapy has been established as one of the most effective treatments when applying to the thoracic malignancies (Ko et al., 2018; Bradley and Mendenhall, 2018). However, this therapy inevitably caused adverse effects as it could damage healthy tissues in the radiation field. It has been reported that 5%-15% patients suffer from radiation induced lung injury (RILI) after thoracic radiation (Giuranno et al., 2019; Hanania et al., 2019). In clinical, RILI can develop into radiation pneumonia in the acute phase or radiation pulmonary fibrosis.

Recently, emerging studies had concentrated on the potentiality of stem cells for treatment of lung-associated diseases, including RILI (Zanoni et al., 2019; Jones-Freeman and Starkey, 2020; Mobius and Thebaud, 2016). In addition, resistance to radiation and potential regeneration capacity had been defined as one of traits of stem cells in mouse models (Barker, 2014). Hence, stem cell biology seems to provide a feasible strategy to reduce radiation damage. However, the underlying molecular mechanisms modulating stem cells maintenance and regeneration during the radiation are largely unknow. Significant contribution to new interventions for protecting from damage and promoting the repair of radiation induced lung injury could be made after elucidating these genetic and cellular mechanisms.

Over the past decade, big strides have been made in the identification of stem cell and how they contribute to regenerate and repair. SOX9, a member of sry-box-containing (SOX) family proteins, has been identified as a stem cell biomarker by lineage tracing in different organs (Wang et al., 2019; Domenici et al., 2019). For instance, SOX9 is required for hair induction and directs the outer root sheath cell to differentiate (Vidal et al., 2005). More importantly, ablation of SOX9 combined with lineage tracing in intestinal epithelium demonstrated that SOX9 could impart mice intestinal stem cell radiation resistance (Roche et al., 2015).

Previous studies showed that SOX9 plays a regenerative role in pulmonary epithelial cells(Laughney et al., 2020; Nichane et al., 2017), showing that SOX9 may regulate proliferative ability after radiation injury. Nevertheless, whether Sox9-expressing cells functions as stem cells in RILI and endows with radiation resistance and regeneration remains unclear.

In our study, we depicted an undefined role of Sox9-expressing cells in the repair and regeneration during RILI. Our results show that the number of Sox9-expressing cells was increased after radiation-induced lung damage. And Sox9-expressing cells were indispensable for repair and reconstruction. Single-cell RNA sequencing (scRNA-Seq) analysis found PI3K/AKT pathway was elevated in Sox9 high-expressing cells. Blocking of PI3K/AKT using small molecular inhibitor greatly repress the regenerative ability of Sox9-expressing cells. Taken together, our provide data show that Sox9-expressing cells is an important factor in repair and regeneration of radiation-induced lung injury.

2. Materials And Methods

2.1. Mice Models. $SOX9^{CreER}$, $Rosa^{tdTomato}$ and $Rosa^{DTA}$ mice were from The Jackson Laboratory. For lineage tracing, $SOX9^{CreER}$, $Rosa^{tdTomato}$ mice were intraperitoneally injected with tamoxifen (Sigma, T5648-1G) at 0.08 mg/g body weight every day for three consecutive days. After radiation treatment (Rs2000, USA), $SOX9^{CreER}$, $Rosa^{tdTomato}$ and $Rosa^{DTA}$ mice were sacrificed at different time points of 3, 7, 14 and 30 days. For PI3K/AKT inhibitor treatment, radiated $SOX9^{CreER}$, $Rosa^{tdTomato}$ mice were assigned into control and Perifosine (250mg/kg mouse weight per week, Beyotime, SC0227) treatment group. After treating for 2 weeks, lung samples were collected at different time points of 3, 7 and 14 days and injected with EdU 2 hours prior to euthanasia. All the animal experiments were proceeded as the Institutional Animal Care and Use Committee-approved protocols.

2.2. Hematoxylin and Eosin Staining. Lung specimens from mice of knockout and control groups were harvested, fixed in 4% paraformaldehyde (biosharp, BL539A) for over 24 hours at 4°C. Later after washed by PBS, samples were dehydrated in gradient ethanol and embedded in paraffin. Then, paraffin sections (3–5μm) of lung tissue were stained as the standard protocol (Solarbio, G1120-100). In brief, slides were then stained with hematoxylin (2 minutes), differentiated with 1% hydrochloric acid ethanol (5 seconds), stained in eosin (1 minutes), followed by ethanol dehydration and neutral balsam medium seal.

2.3. Immunohistochemical staining and IHC score. For immunological analyses, 3–5 μm microtome sections were deparaffinizing for 30 minutes and rehydrating with gradient alcohol. Then, the endogenous peroxidase of sections was consumed in 3% H_2O_2 followed by heat-induced epitope retrieval. The primary antibody incubation was at 4°C overnight in the following concentrations: SOX9 (1:200; CST, 82630S), Ki67 (1:500; Proteintech, 27309), CD45 (1:200; Abcam, ab10559), α-SMA (1:200; Abcepta, AD80141), and Caspase-3 (1:200; SAB, 27525). The specimens were washed by phosphate-buffered saline (PBS) for three times prior to anti-primary secondary antibody incubation for 30 minutes at 37°C. For enzymatic methods, horseradish peroxidase (HRP) conjugate was used for detection. IHC score was defined by multiplying the percentage of positive cells by the intensity. And the intensity was scored as 0 (negative), 1+ (weakly staining), 2+ (moderate staining) or 3+ (strongly staining) while the frequency was scored according to the proportion of positive cells.

2.4. Immunofluorescence staining. Tissues were fixed in 4% paraformaldehyde and treated with Triton X-100 (Sigma, US) permeabilization buffer. Following treatment, lung specimens were blocked with PBS containing 1% bovine serum at room temperature and incubated with primary antibody at 4°C. DyLight 488 and Fluor 594 (Invitrogen, US) was stained for 1 hour at room temperature, after which cell nucleus was identified by DAPI staining at 1:1000 for 1 minute. Images were obtained with a fluorescence microscopy.

2.5. Masson's trichrome staining. Dewaxing and rehydrating sections were acquired according to the same process described above. In order to evaluate the degree of fibrosis and lesion localization, Masson's trichrome staining was performed following the standard protocol (G1343, Solarbio).

2.6. Single-Cell Analysis. The scRNA-seq data of mouse tracheal epithelial cells were used in this study for analysis. A total of 7,662 cells scRNA-seq data, GEO number GSE102580 (Plasschaert et al., 2018), was acquired from the Gene Expression Omnibus (GEO, http://www.ncbi.nlm.nih.gov/geo/) database. The data was analyzed using Seurat R package.

2.7. Statistical Analysis. Statistical analysis of all data was carried out by GraphPad Prism 8.0. The data are expressed as mean ± standard deviation (SD). Statistical significance was analyzed by two-tailed unpaired Students t-test. $P < 0.05$ was considered to be significant.

3. Results

3.1. Sox9-expressing cells contribute to the regeneration of lung after radiation

To characterize the expression of Sox9 in the mouse adult lung tissue, we first performed IHC assay on normal lung tissues. We found that Sox9 protein was sparsely expressed in the bronchus while barely detectable in the alveoli of the adult mouse lung (Fig. 1A). However, we observed elevated level of Sox9 protein in the bronchus 3 days after radiation (Fig. 1A). Surprisingly, we also noticed expression of Sox9 in the alveoli region 3 days after radiation (Fig. 1A). To investigate the role of Sox9 expressing cells during lung homeostasis and healing process after radiation, we carried out lineage tracing assay using *Sox9*^{creER}; *Rosa*^{Tomato} transgenic mice (Fig. 1B). Consistent with the IHC results, our lineage tracing data show that Tomato^{+} cells were located in normal lung epithelium but not in the alveoli region (Fig. 1B). When we traced these cells for 30 days in normal homeostasis condition, we found that the number of Tomato^{+} cells remained constant compared with 3 days (Fig. 1B), suggesting Sox9-expressing cells in the bronchus have limited function during normal lung homeostasis.

To test whether Sox9-expressing cells play a role in radiation-induced lung regeneration, *Sox9*^{creER}; *Rosa*^{Tomato} mice were first given Tamoxifen and received 15 Gy of radiation in the lung region (Fig. 1C). After radiation treatment, immunofluorescent staining results showed Sox9-expressing cells in both bronchus and alveoli cells were obviously increased (Fig. 1D, E). And the number of Sox9-expressing cells in the bronchus gradually increased over time after radiation (Fig. 1D). Similarly, we observed expansion of Tom^{+} cell colonies which can differentiated into both PDPN positive alveolar type I cells and PDPN negative alveolar cells. Taken together, our data indicate that Sox9-expressing cells can contribute to the lung regeneration after radiation.

3.2. Sox9-expressing cells is essential for the regeneration of lung after radiation

To further interrogate the specific role of Sox9-expressing cells during lung regeneration after radiation, we generated *Sox9*^{CreER}; *Rosa*^{Tomato}; *Rosa*^{DTA} mice that allow for Tamoxifen-inducible expression of diphtheria toxin A (DTA) enabling targeted ablation of Sox9 expressing cells (Fig. 2A). To examine the morphological changes of lung in mice after ablation of Sox9 expressing cells during radiation induced regeneration, the *Sox9*^{CreER}; *Rosa*^{Tomato}; *Rosa*^{DTA} mice and *Sox9*^{CreER}; *Rosa*^{Tomato} transgenic littermates were subjected to histological examination. Our H&E staining results demonstrated that mouse lung tissue without Sox9-expressing cells displayed thickening of the alveolar septa and disruption of the integrity of pulmonary alveoli compared with the control group after radiation (Fig. 2B), suggesting a loss of regenerative capacity. The lineage tracing results confirmed that the majority of Sox9 expressing cells were ablated after Tamoxifen administration (Fig. 2C, D). Furthermore, ablation of Sox9-expressing cells led to a significantly decreased of proliferating cells and increased apoptosis (Fig. 2E, F) and more severe lung inflammatory infiltration level (Fig. 2G). And compared with control groups, ablation of Sox9-

expressing cells aggravated the radiation-induced pulmonary fibrosis (Fig. 2H, I). These data indicate the essential role of Sox9-expressing cells in the regeneration and repair of lung after radiation in vivo.

3.3 Sox9 maintains regenerative ability of stem cells via AKT/PI3K pathway

To further investigate the underlying mechanism of Sox9 expressing cells during lung regeneration, we analyzed an online single cell RNA-seq dataset which characterized the cellular composition of mouse regenerating lung epithelium after polidocanol-induced injury (GSE102580) (Plasschaert et al., 2018). We first examined the expression of Sox9 in cycling basal keratinocytes, which are responsible for lung epithelium regeneration. In accord with our above findings, we found Sox9 was up-regulated in a subset of cycling basal keratinocytes using online dataset (Fig. 3A). We then divided the cycling basal keratinocytes into $Sox9^{+}$ and $Sox9^{-}$ population based on their Sox9 expression levels. We used Seurat R package to determine the differentially expressed genes between these two populations using a Wilcoxon Rank Sum test. We found 117 genes were significantly elevated in the $Sox9^{+}$ population. KEGG pathways analysis of these genes showed enrichment pathways, including cell cycle, focal adhesion, PI3K-Akt signaling pathway, ECM-receptor interaction and Wnt signaling pathway (Fig. 3B). Indeed, we found dramatic down regulation of PI3K-Akt signaling pathway downstream targets, such as Ccnd1, Cdk6, Lamc2, Myc, Pdgfa and Tnc (Fig. 3C). We then examined whether Sox9 expressing cells co-expressed previous known lung epithelium stem cells markers. Surprisingly, we detected no difference in the expression of Sox2, Krt14, Krt5 and Trp63 between $Sox9^{+}$ and $Sox9^{-}$ population (Fig. 3D), suggesting Sox9 expressing cells were not overlap with previous identified lung epithelium stem cells populations.

3.4. AKT/PI3K pathway inhibitor could attenuate the effect

Finally, to probe the possible functional role of PI3K-Akt signaling pathway in regulating Sox9 expressing cells during radiation-induced lung regeneration, we used Perifosine, a specific AKT inhibitor, to treat mice after radiation damage. As shown in the Fig. 5A and 5B, after treatment of Perifosine, alveolar septum was thickened and pulmonary fibrosis was deteriorated. Similarly, the proliferation of pulmonary epithelial cells was significantly reduced (Fig. 5C). And lineage tracing assay results show that Sox9 expressing cells were incapable to differentiate into functional cells like the control group (Fig. 5D and 5E). Therefore, our data indicated that the regeneration and repair of Sox9 expressing cells after radiation injury is controlled by the PI3K/AKT signaling pathway.

4. Discussion

RILI, including radiation pneumonia and radiation pulmonary fibrosis, was characterized of inflammatory phenotype and cell repair disorder (Lu et al., 2019). And it is worth noting that emerging evidence emphasizes the participation of stem cells in RILI, providing new perspective for obtaining better efficacy. In our study, data has showed the profound role of Sox9 expressing cells in repair and regeneration in response to irradiation via PI3K/AKT signaling pathway.

Recently, new researches focused on stem cells have shed light on how to utilize unique molecule marker to identify regenerative ability cells (Hatina et al., 2018; Yu et al., 2016). Experimental analysis such as transcriptome, proteomics and lineage tracing has proved that many biomarkers attribute to a certain stem cell population (Ragelle et al., 2017; Munoz et al., 2012; Yan et al., 2017). Data showed that Sox9 expressing cells were rare but they are a requisite for regeneration after RILI. In addition to manipulate lung cell proliferation, we found alveolar epithelial cells turned into radiosensitive after Sox9 expressing cells were ablated. In addtion, Sox9 expressing cells ablation in lung tissue suffered from severer lesions, showing higher levels of inflammation and more extensive fibrosis. Notably, despite our data verified Sox9 expressing cells played a key role in irradiation resistance, the specific mechanism in which Sox9 expressing cells participate need further analysis.

We found that Sox9 expressing cells are endowed with regenerative phenotype after RILI. Subsequently, the specific mechanism that Sox9 expressing cells participated in cell proliferation have been analyzed by the scRNA-seq data. Notably, Sox9 expressing cells differentially upregulated genes were significantly enriched in the PI3K/AKT signaling pathway. Previous studies have shown that repressed PI3K/AKT signaling pathway predisposed cells to reduced DNA repair capacity, resulting in an increase of radiation-induced apoptosis (Liao et al., 2019). Consistent with a radio-resistant phenotype, another study demonstrated that PI3K/AKT dependent pathways play a protective or promoting regenerative role after radiation injury (Yang et al., 2014). And recent advances in pathway studies showed SOX9 could activate PI3K/AKT signaling pathway and promoted cellular proliferation (Chang et al., 2015; Wang et al., 2020), both of which indicated its potential in regeneration and repair. Based on the above results, in vivo AKT inhibitors assay results further confirmed our hypothesis, inactivation of AKT pathway has been shown to decrease cellular proliferation and Sox9 expressing cells fail to differentiate. Taken together, these studies support the explanation that Sox9 expressing cells are involved in regeneration and repair by activating PI3K/AKT signaling pathway after RILI.

5. Conclusion

To sum up, our study provides a model in which Sox9 expressing cells serves as a functional cell population in pulmonary epithelial cells and imparts regeneration and reestablish capacity to stem cells through promoting PI3K/AKT pathway. Despite the fact that radiation-induced lung injury, one of the common injuries of chest radiotherapy, has brought challenges to patients' quality of life and disease prognosis for a long time, it is by no means a scourge.

Abbreviations

RILI
Radiation induced lung injury
SOX
a member of sry-box-containing
scRNA-Seq

Single-cell RNA sequencing
PBS
phosphate-buffered saline
HRP
horseradish peroxidase
GEO
Gene Expression Omnibus
SD
standard deviation
DTA
diphtheria toxin A
Tam
tamoxifen

Declarations

Data Availability

The data used to support the findings of this study are available from the corresponding author upon request.

Ethics declarations

Ethics approval and consent to participate

All the animal experiments were proceeded as the Institutional Animal Care and Use Committee-approved protocols.

Consent for publication

Not applicable.

Competing interests

The authors indicate no competing interests.

Acknowledgments

The authors acknowledge the team of Plasschaert at Novartis Institutes for BioMedical Research which gave public access to their transcriptome data under Gene Expression Omnibus access number GSE102580.

Funding

This paper was supported by the KEY PROJECT (BWS18J008), Natural Science Foundation of China (No. 81974443) and Natural Science Foundation of Guangdong Province (No. 2018A030313176).

Author Contributions

DC, HP and LP conceived and designed this project. SC and KL conducted experiments and interpreted results of experiments. GPW and XCW drafted paper, edited and revised manuscript. MSC, JC and ZC perform data analysis. CHZ, GX, JWC and XX prepared figures. All authors read and approved the final manuscript.

References

Barker, N. (2014). Adult intestinal stem cells: critical drivers of epithelial homeostasis and regeneration. Nat Rev Mol Cell Biol *15*, 19-33.

Bradley, J.A., and Mendenhall, N.P. (2018). Novel Radiotherapy Techniques for Breast Cancer. ANNU REV MED *69*, 277-288.

Chang, L., Graham, P.H., Ni, J., Hao, J., Bucci, J., Cozzi, P.J., and Li, Y. (2015). Targeting PI3K/Akt/mTOR signaling pathway in the treatment of prostate cancer radioresistance. Crit Rev Oncol Hematol *96*, 507-517.

Domenici, G., Aurrekoetxea-Rodriguez, I., Simoes, B.M., Rabano, M., Lee, S.Y., Millan, J.S., Comaills, V., Oliemuller, E., Lopez-Ruiz, J.A., and Zabalza, I.*, et al.* (2019). A Sox2-Sox9 signalling axis maintains human breast luminal progenitor and breast cancer stem cells. ONCOGENE *38*, 3151-3169.

Feng, R.M., Zong, Y.N., Cao, S.M., and Xu, R.H. (2019). Current cancer situation in China: good or bad news from the 2018 Global Cancer Statistics? Cancer Commun (Lond) *39*, 22.

Giuranno, L., Ient, J., De Ruysscher, D., and Vooijs, M.A. (2019). Radiation-Induced Lung Injury (RILI). FRONT ONCOL *9*, 877.

Hanania, A.N., Mainwaring, W., Ghebre, Y.T., Hanania, N.A., and Ludwig, M. (2019). Radiation-Induced Lung Injury: Assessment and Management. CHEST *156*, 150-162.

Hatina, J., Parmar, H.S., Kripnerova, M., Hepburn, A., and Heer, R. (2018). Urothelial Carcinoma Stem Cells: Current Concepts, Controversies, and Methods. Methods Mol Biol *1655*, 121-136.

Jones-Freeman, B., and Starkey, M.R. (2020). Bronchioalveolar stem cells in lung repair, regeneration and disease. J PATHOL *252*, 219-226.

Ko, E.C., Raben, D., and Formenti, S.C. (2018). The Integration of Radiotherapy with Immunotherapy for the Treatment of Non-Small Cell Lung Cancer. CLIN CANCER RES *24*, 5792-5806.

Laughney, A.M., Hu, J., Campbell, N.R., Bakhoum, S.F., Setty, M., Lavallee, V.P., Xie, Y., Masilionis, I., Carr, A.J., and Kottapalli, S.*, et al.* (2020). Regenerative lineages and immune-mediated pruning in lung cancer metastasis. NAT MED *26*, 259-269.

Liao, J., Jin, H., Li, S., Xu, L., Peng, Z., Wei, G., Long, J., Guo, Y., Kuang, M., and Zhou, Q.*, et al.* (2019). Apatinib potentiates irradiation effect via suppressing PI3K/AKT signaling pathway in hepatocellular carcinoma. J Exp Clin Cancer Res *38*, 454.

Lu, L., Sun, C., Su, Q., Wang, Y., Li, J., Guo, Z., Chen, L., and Zhang, H. (2019). Radiation-induced lung injury: latest molecular developments, therapeutic approaches, and clinical guidance. CLIN EXP MED *19*, 417-426.

Mobius, M.A., and Thebaud, B. (2016). Cell Therapy for Bronchopulmonary Dysplasia: Promises and Perils. PAEDIATR RESPIR REV *20*, 33-41.

Munoz, J., Stange, D.E., Schepers, A.G., van de Wetering, M., Koo, B.K., Itzkovitz, S., Volckmann, R., Kung, K.S., Koster, J., and Radulescu, S.*, et al.* (2012). The Lgr5 intestinal stem cell signature: robust expression of proposed quiescent '+4' cell markers. EMBO J *31*, 3079-3091.

Nichane, M., Javed, A., Sivakamasundari, V., Ganesan, M., Ang, L.T., Kraus, P., Lufkin, T., Loh, K.M., and Lim, B. (2017). Isolation and 3D expansion of multipotent Sox9(+) mouse lung progenitors. NAT METHODS *14*, 1205-1212.

Plasschaert, L.W., Zilionis, R., Choo-Wing, R., Savova, V., Knehr, J., Roma, G., Klein, A.M., and Jaffe, A.B. (2018). A single-cell atlas of the airway epithelium reveals the CFTR-rich pulmonary ionocyte. NATURE *560*, 377-381.

Ragelle, H., Naba, A., Larson, B.L., Zhou, F., Prijic, M., Whittaker, C.A., Del, R.A., Langer, R., Hynes, R.O., and Anderson, D.G. (2017). Comprehensive proteomic characterization of stem cell-derived extracellular matrices. BIOMATERIALS *128*, 147-159.

Roche, K.C., Gracz, A.D., Liu, X.F., Newton, V., Akiyama, H., and Magness, S.T. (2015). SOX9 maintains reserve stem cells and preserves radioresistance in mouse small intestine. GASTROENTEROLOGY *149*, 1553-1563.

Vidal, V.P., Chaboissier, M.C., Lutzkendorf, S., Cotsarelis, G., Mill, P., Hui, C.C., Ortonne, N., Ortonne, J.P., and Schedl, A. (2005). Sox9 is essential for outer root sheath differentiation and the formation of the hair stem cell compartment. CURR BIOL *15*, 1340-1351.

Wang, L., Zhang, Z., Yu, X., Huang, X., Liu, Z., Chai, Y., Yang, L., Wang, Q., Li, M., and Zhao, J.*, et al.* (2019). Unbalanced YAP-SOX9 circuit drives stemness and malignant progression in esophageal squamous cell carcinoma. ONCOGENE *38*, 2042-2055.

Wang, L., Zhang, Z., Yu, X., Li, Q., Wang, Q., Chang, A., Huang, X., Han, X., Song, Y., and Hu, J.*, et al.* (2020). SOX9/miR-203a axis drives PI3K/AKT signaling to promote esophageal cancer progression. CANCER LETT *468*, 14-26.

Yan, K.S., Gevaert, O., Zheng, G., Anchang, B., Probert, C.S., Larkin, K.A., Davies, P.S., Cheng, Z.F., Kaddis, J.S., and Han, A.*, et al.* (2017). Intestinal Enteroendocrine Lineage Cells Possess Homeostatic and Injury-Inducible Stem Cell Activity. CELL STEM CELL *21*, 78-90.

Yang, L., Wang, R., Gao, Y., Xu, X., Fu, K., Wang, S., Li, Y., and Peng, R. (2014). The protective role of interleukin-11 against neutron radiation injury in mouse intestines via MEK/ERK and PI3K/Akt dependent pathways. Dig Dis Sci *59*, 1406-1414.

Yu, Q.C., Song, W., Wang, D., and Zeng, Y.A. (2016). Identification of blood vascular endothelial stem cells by the expression of protein C receptor. CELL RES *26*, 1079-1098.

Zanoni, M., Cortesi, M., Zamagni, A., and Tesei, A. (2019). The Role of Mesenchymal Stem Cells in Radiation-Induced Lung Fibrosis. INT J MOL SCI *20*.

Figures

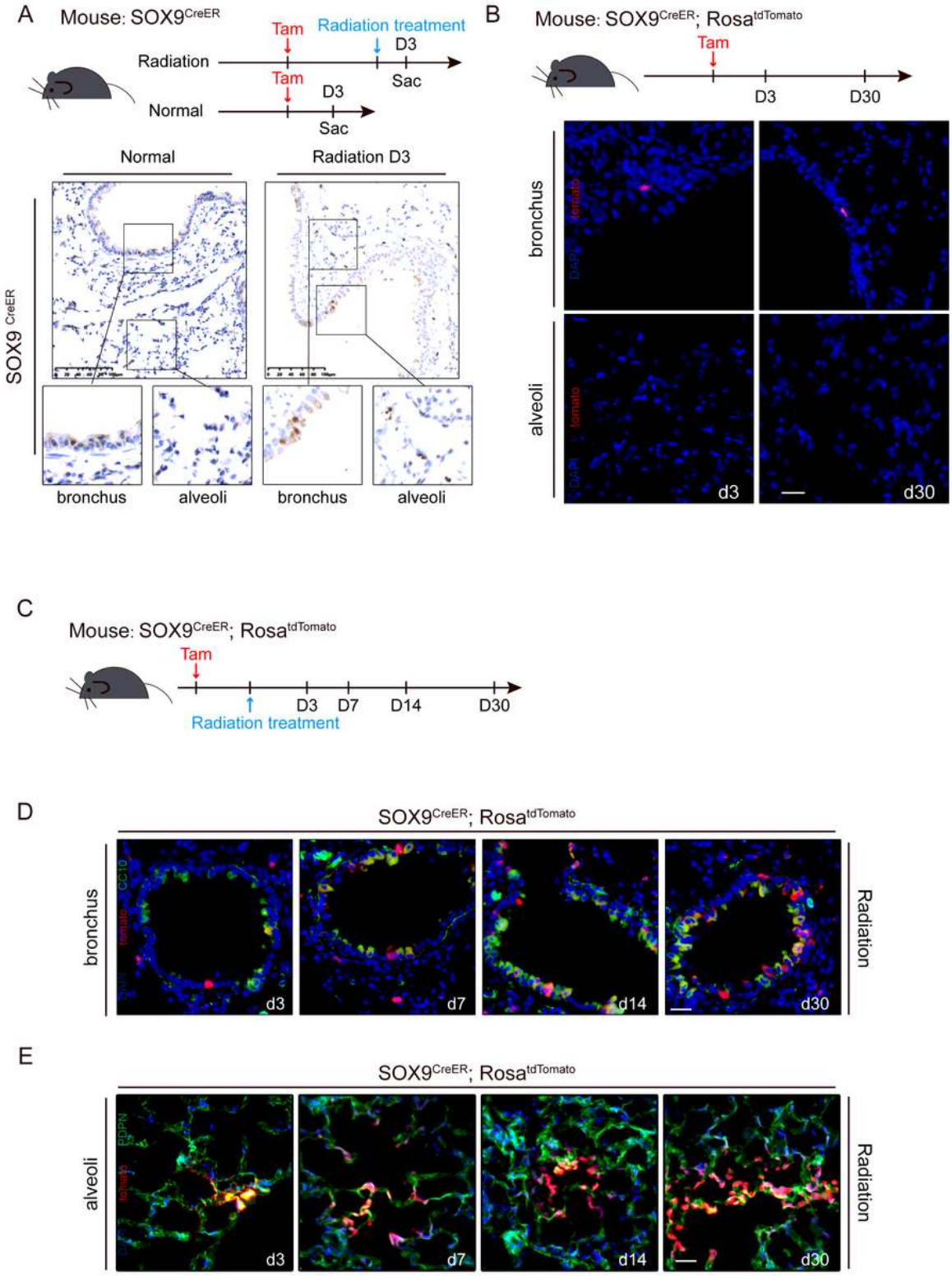

Figure 1

Sox9-expressing cells contribute to the regeneration of lung after radiation A. Upper; experimental design for control and radiation group. Lower; representative IHC staining images of SOX9 for control group (left) and after radiation damage group (right) in SOX9CreER mice. Lung tissues were collected after 3 days after radiation treatment. Scale bar, 100 μm. B. Upper; experimental design for SOX9+ cells lineage tracing for control and radiation group. Lower; representative images of lineage tracing in lung tissue

sections under homeostasis condition. Nuclei were stained with DAPI (blue). Lung tissues were collected after 3 and 30 days after radiation treatment. Scale bar, 50 μm. C. Experimental design for SOX9+ cells lineage tracing of SOX9CreER; RosatdTomato mice after treatment with radiation. Before treatment, the mice were injected with tamoxifen (Tam). Mice were sacrificed at time of 3, 7, 14 and 30 days after radiation treatment. D. Representative images of SOX9+ cell-driven lineage tracing in bronchus of SOX9CreER; RosatdTomato after radiation injury. Nuclei were stained with DAPI (blue). Lung tissues were collected after 3, 7, 14 and 30 days after radiation treatment. Scale bar, 50 μm. E. Representative images of SOX9+ cell-driven lineage tracing in alveoli of SOX9CreER; RosatdTomato mice after radiation injury. Nuclei were stained with DAPI (blue). Lung tissues were collected after 3, 7, 14 and 30 days after radiation treatment. Scale bar, 50 μm.

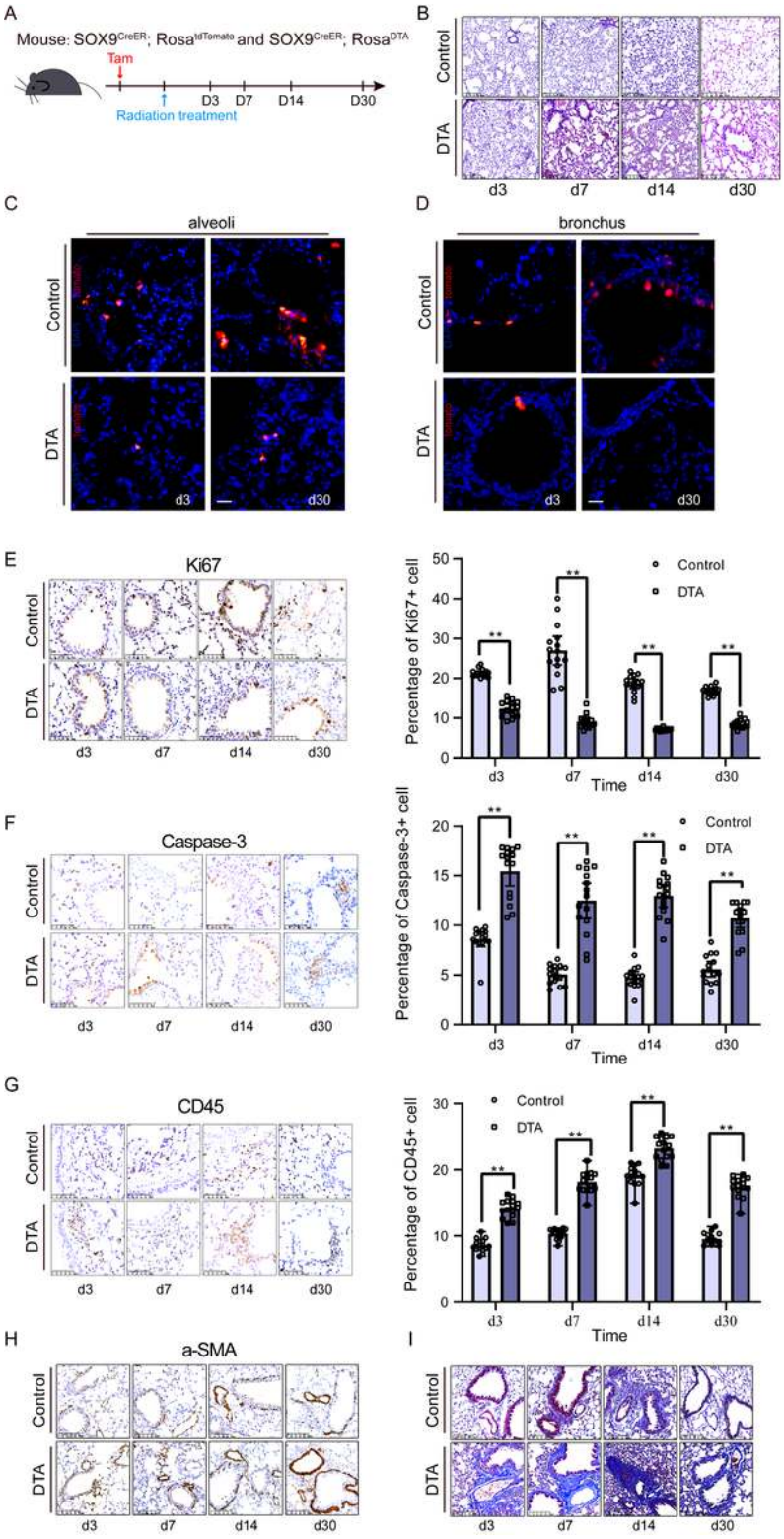

Figure 2

Sox9-expressing cells is essential for the regeneration of lung after radiation A. Experimental design for SOX9 knockout and control group lineage tracing after treatment with radiation (n = 4 per group). Before treatment, the mice were injected with tamoxifen (Tam). Mice were sacrificed at time of 3, 7, 14 and 30 days after radiation treatment. B. Representative images of H&E staining of lung tissue section in SOX9 knockout and control mice. Scale bar, 100 μm. C. and D. Immunostaining images of SOX9+ cell-driven

lineage tracing in alveoli and bronchus of SOX9 knockout and control group. Scale bar, 50 μm. E. F. and G. Representative IHC staining images of ki67, Caspase-3, and CD45 after radiation damage in SOX9CreER; RosaDTA mice and control group (left). IHC staining scores of ki67, CD45 and Caspase-3 were counted (right) respectively. ∗p<0.05, ∗∗p<0.01, and ∗∗∗p<0.001. Scale bar, 100 μm. H. Immunostaining of a-SMA in SOX9CreER; RosaDTA mice and control group. Scale bar, 100 μm. I. Representative images of Masson's trichrome staining in SOX9CreER; RosaDTA mice and control group. Scale bar, 100 μm.

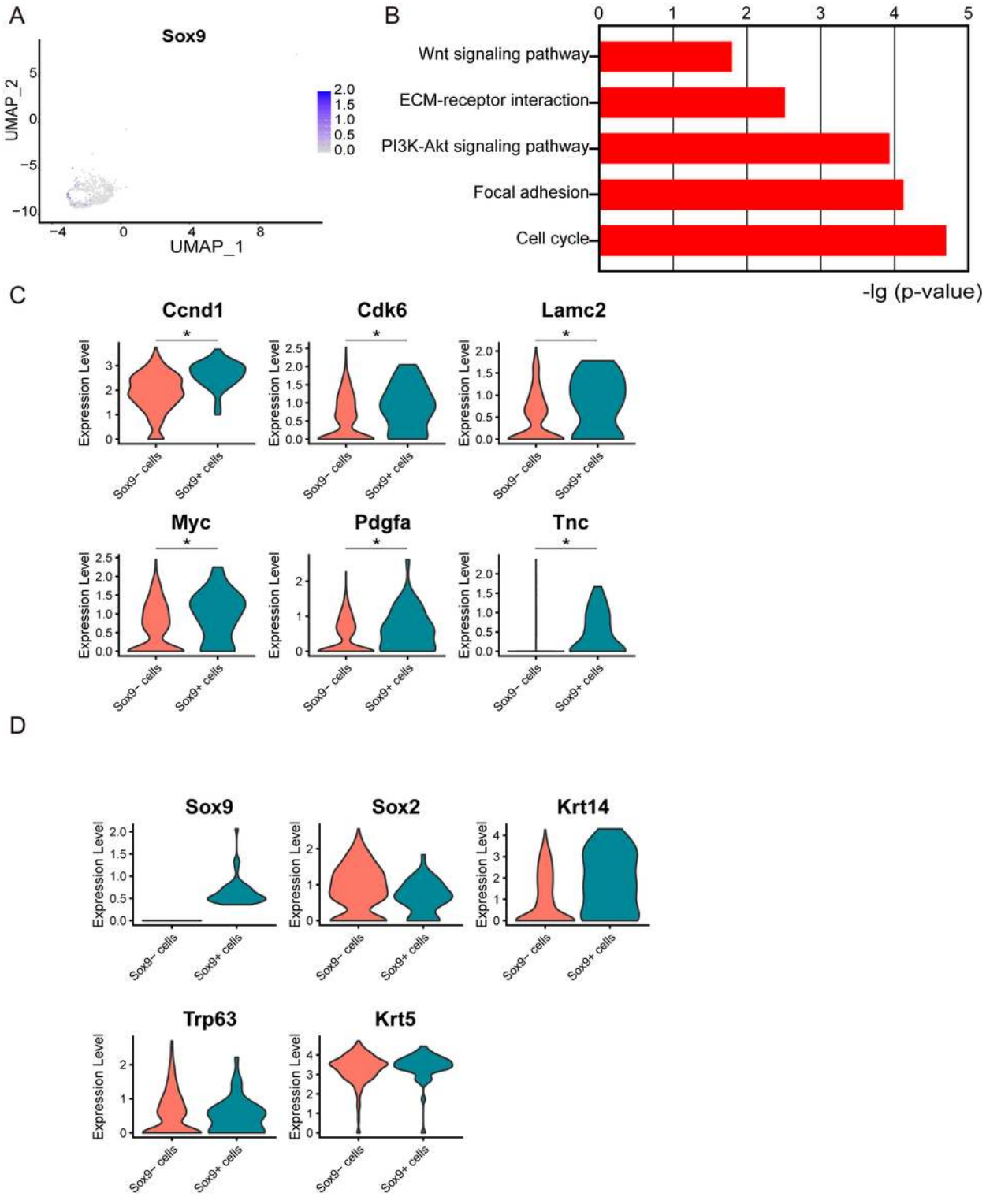

Figure 3

Sox9 maintains regenerative ability of stem cells via AKT/PI3K pathway A. Dot plots showing the pattern of SOX9 expression for the cell cluster on the UMAP map. B. Enrichment of different KEGG pathways using the SOX9 co-expressing genes from the scRNA-seq data. C. Violin plots that depict the expression of indicated PI3K/Akt downstream target genes for Sox9+ and Sox9- cells. ∗p<0.05, ∗∗p<0.01, and ∗∗∗p<0.001. D. Violin plots that depict the expression of indicated known stem cell markers for Sox9+ and Sox9- cells.

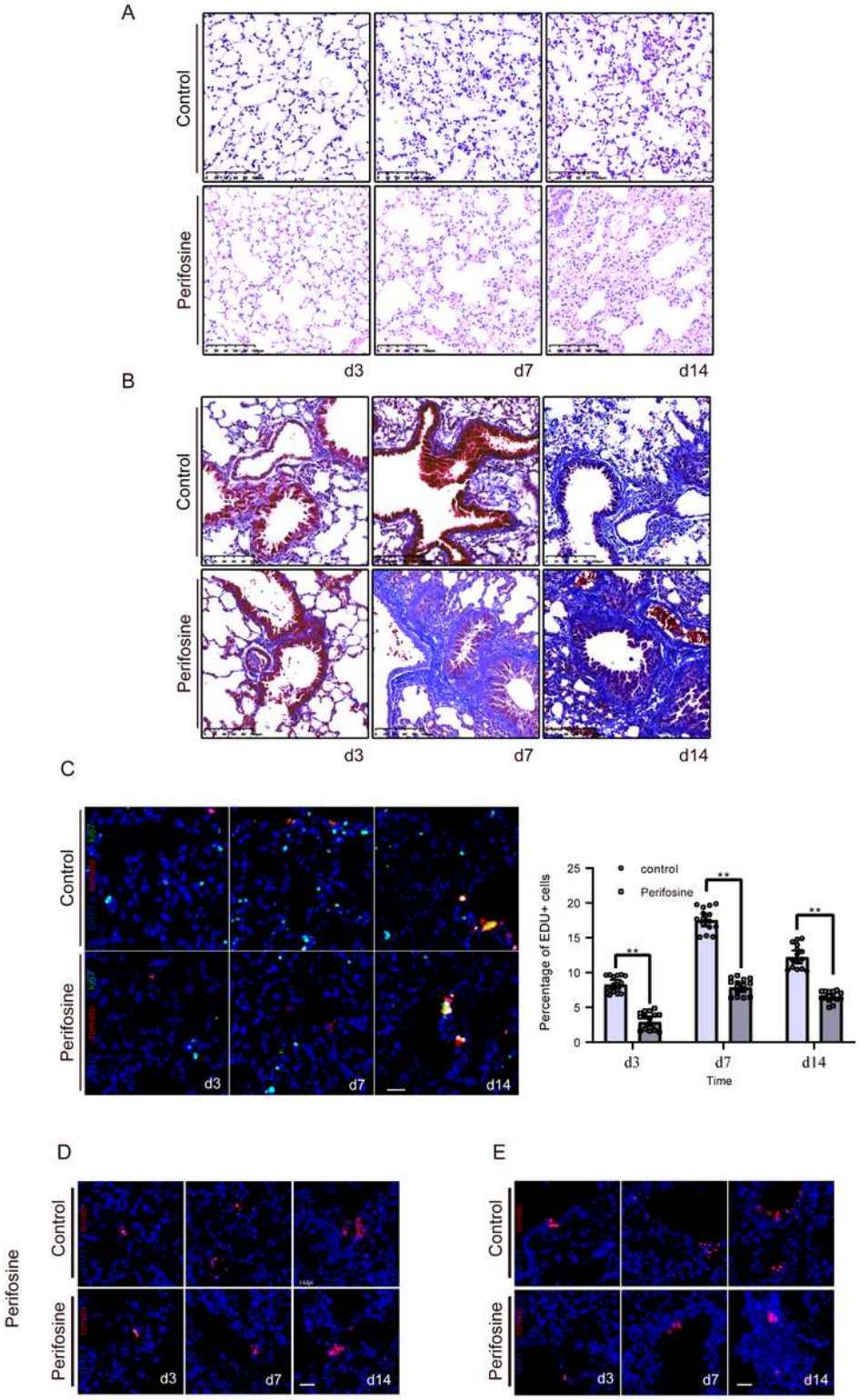

Figure 4

AKT/PI3K pathway inhibitor could attenuate the effect A. Representative images of H&E staining of lung tissue section in SOX9CreER; RosatdTomato mice after RILI. And AKT inhibitor was intragastric administration after radiation damage. Lung tissues were collected after 3,7 and14 days after drug treatment. Scale bar, 100 μm. B. Representative images of Masson's trichrome staining in AKT inhibitor group and control group. Scale bar, 100 μm. C. Immunostaining of EdU+ cells in SOX9CreER; RosatdTomato mice after RILI and the inhibitor treatment. Staining score of EdU+ cells were counted (right). $*p<0.05$, $**p<0.01$, and $***p<0.001$. Scale bar, 50 μm. D. and E. Representative images of SOX9+ cell-driven lineage tracing in mice after radiation injury and inhibitor treatment. Nuclei were labeled with DAPI (blue). Scale bar, 50 μm.